

# Evaluation of Light-Scattering Detectors for Size Exclusion Chromatography. II. Light-Scattering Equation Selection

L. JENG and S. T. BALKE\*

Department of Chemical Engineering and Applied Chemistry, University of Toronto,  
Toronto, Ontario, M5S 1A4, Canada

## SYNOPSIS

A new multiangle laser light-scattering (MALLS) detector for size exclusion chromatography promises simultaneous measurement of both weight-average molecular weight ( $M_w$ ) and radius of gyration ( $r_g$ ) at each retention volume across the chromatogram. However, there are a variety of ways of interpreting the raw data to provide these results. This study examines variations of three different rearrangements of the basic light-scattering equation. Data from a room temperature analysis of polystyrene and a high-temperature analysis of polyethylene were used. The degree of fit of each equation to the data and the precision of the  $M_w$  and  $r_g$  values are evaluated. To define precision, joint confidence regions (JCRs) were calculated and compared to simple confidence intervals based upon standard deviations in order to see the effect of interdependence of  $M_w$  and  $r_g$ . Results showed that the Debye equation was superior to the inverse Debye equation (similar to the Zimm plot) for the interpretation of MALLS data. The effect of the quantity of data included in the regression model was also assessed. Use of only the most precise four detector angles was compared to use of a full set of 15 angles. Precision of weight-average molecular weight values was found to be improved as the detector angle decreased because of the shortened extrapolation to zero angle. Precision at room temperature was much superior to that at high temperature. Use of simple confidence intervals was shown to provide only a fair approximation to the more accurate JCR. The "natural scatter" of data shown by the JCR generally shows the same trend as do plots in the literature of  $M_w$  vs.  $r_g$ . Thus, it is concluded that JCRs should be more often calculated in light-scattering studies in order to distinguish random scatter from meaningful correlations of these values. © 1993 John Wiley & Sons, Inc.

## INTRODUCTION

In Part I of this series, the instrument precision and accuracy of the Chromatix KMX 6 (LALLS) and the Wyatt Dawn-F multiangle laser light-scattering (MALLS) detector were evaluated. MALLS can provide both  $M_w$  and  $r_g$  at each retention volume<sup>†</sup> because it can determine the angular dependence of

scattered light by measuring scattered light at each of 15 different angles simultaneously.<sup>1</sup> However, there are many different computational options available to obtain these results.

This paper assesses some of these by examining their degree of fit to the data and the precision of the results obtained. Some of our earlier results in this area have recently been published.<sup>2</sup> In the next section, the options to be examined are detailed and the statistical methods of comparison are described.

## COMPUTATIONAL OPTIONS IN MALLS

The presence of "computational options" refers to the fact that the same two local values,  $M_w$  and  $r_g$ , at each retention volume can be calculated from the MALLS data in different ways. Both the accuracy

\* To whom correspondence should be addressed.

† Note that this paper deals only with local values of weight-average molecular weight and radius of gyration (actually the z-average root mean square radius of gyration). By local values is meant the values at a particular retention volume (i.e., for a particular molecular size fractionated by the chromatograph). These values should be distinguished from the "whole polymer" or "overall" values,  $\bar{M}_w$  and  $\bar{r}_g$  (see Part I).

(closeness to truth) and precision (repeatability) of the values obtained can be affected by the option selected.

In this paper, these options originate from four sources:

- (i) A subset of the main body of data can be selected for calculation. For example, the most precise four angles can be used (instead of all 15 angles).
- (ii) Different series approximations can be used. As will be seen below, one equation utilizes a series expression for the angular dependence of scattered light, while another utilizes an series expression for the inverse dependence.
- (iii) Additional terms can be retained in series approximations contained in the light-scattering equations. For example, higher terms can be retained in the expression for the angular dependence of scattered light.
- (iv) The criterion used for accepting a fit of an equation to the data can result in different values of  $M_w$  and  $r_g$  with different reproducibility obtained from the same equations. The complication here is that light scattering has evolved based upon graphical methods. Equations have been rearranged in different ways to obtain straight lines when plotted so that they can be readily extrapolated to zero. Rearrangement of an equation produces a group of measured quantities that is to be calculated at each angle and plotted. The error in such a group can be much greater than the error in the individual measured quantities because of "error propagation" and may be a strong function of the angle. In applying computer-fitting methods, such as least squares, to fit the plots, this variation in error needs to be taken into account in order to obtain the best obtainable accuracy and precision in the estimates of  $M_w$  and  $r_g$ . If an incorrect weighting is used, a systematic error in the fit can result as well as inaccuracy and imprecision in these estimates. Correct weighting factors can be obtained by applying the error propagation equation to the group in order to derive an expression for the error variance of the group as a whole.

In this paper, three different rearrangements of the basic light-scattering equation used for fitting MALLS data are examined. The paper then pro-

ceeds to examine the adequacy of the fit and precision of the estimated  $M_w$  and  $r_g$  values for each when used with the data. Accuracy generally cannot be estimated since the true values are not known. The three equation rearrangements and the computational options resulting are summarized in the following paragraphs.

### The Debye Plot Equation

Conventional interpretation of MALLS to obtain  $M_w$  and  $r_g$  depends upon construction of a Debye plot<sup>3</sup> at each retention volume [a plot of  $R_\theta/Kc$  vs.  $\sin^2(\theta/2)$ ] based upon

$$\frac{R_\theta(\nu)}{Kc(\nu)} = P(\theta)M_w(\nu) \quad (1)$$

where  $P(\theta)$  represents the angular dependence of the scattered light:

$$P(\theta) = 1 - \frac{16\pi^2 n_0^2 r_g^2(\nu) \sin^2(\theta/2)}{3\lambda_0^2} + \text{higher terms} \quad (2)$$

and  $K$  is the instrument's optical constant:

$$K = \frac{4\pi^2 n_0^2 (dn/dc)^2}{\lambda_0^4 N} \quad (3)$$

for each of the 15 detector angles. Equation (1) assumes that concentrations are sufficiently dilute that terms involving the product of the second virial coefficient, concentration, and  $M_w$  together are negligible.

Linear regression can be used to determine  $M_w$  and  $r_g$  at any specific retention volume by minimizing  $Q$  over the  $n_a$  angles at retention volume  $\nu$ :

$$Q = \sum_{j=1}^{n_a} w_j \left[ \left( \frac{R_{\theta_j}(\nu)}{K c(\nu)} \right)_{\text{exp}} - \left( \frac{R_{\theta_j}(\nu)}{K c(\nu)} \right)_{\text{calc}} \right]^2 \quad (4)$$

where  $w_j$  is a weighting factor equal to the reciprocal of the error variance of the quantity  $[R_{\theta_j}(\nu)/(K c(\nu))]_{\text{exp}}$ . This approach, with  $w_j$  equal to unity at each angle, is used in the commercial software, ASTRA version 1.15 and later versions, offered by Wyatt Technology Corp., Santa Barbara, CA.

However, when the error variance of  $[R_{\theta_j}(\nu)/(K c(\nu))]_{\text{exp}}$  is obtained at a particular value of  $\nu$

from replicate chromatograms, the fluctuation in  $c(v)$  at  $v$  are factored into the estimate along with the variation in  $R_{\theta_j}(v)$ . Only the latter varies with angle  $\theta$ . However, it can be shown that the error variance of the group  $[R_{\theta_j}(v)/(Kc(v))]_{\text{exp}}$  may be greater and may vary more with the angle than will  $R_{\theta_j}(v)$  alone because of the presence of error in the concentration. Since a variation in variance with the angle means a variation of the weighting factor with the angle, the fit may be affected. However, when a fit of  $[R_{\theta_j}(v)/(Kc(v))]_{\text{exp}}$  vs.  $\sin^2(\theta/2)$  is actually carried out at a particular retention volume, the value of concentration used to calculate the group  $[R_{\theta_j}(v)/(Kc(v))]_{\text{exp}}$  is a constant. Then, the random error in concentration appears as a constant difference between the single value of concentration used and the true value. This causes a systematic error, or bias, in the results. Thus, the error in concentration can affect the results in two different ways: through the weighting factors and through bias. If the more traditional weighting factor of unity is used for each term, the error variance of  $[R_{\theta_j}(v)/(Kc(v))]_{\text{exp}}$  for each of the 15 MALLS detectors is assumed to be constant with respect to the scattering angle.

### Inverse Debye Plot Equation

Another alternative for MALLS data interpretation is to plot  $Kc/R_{\theta}$  vs.  $\sin^2(\theta/2)$ . This "inverse Debye plot equation" is based on a rearrangement of eq. (2):

$$\frac{Kc(v)}{R_{\theta}(v)} = \frac{P^{-1}(\theta)}{M_w(v)} \quad (5)$$

where

$$P^{-1}(\theta) = 1 + \frac{16\pi^2 n_0^2 r_g^2(v) \sin^2(\theta/2)}{3\lambda_0^2} + \text{higher terms} \quad (6)$$

To obtain  $M_w$  and  $r_g$ , linear least-squares regression minimizes

$$Q = \sum_{j=1}^{n_a} w_j \left[ \left( \frac{Kc(v)}{R_{\theta_j}(v)} \right)_{\text{exp}} - \left( \frac{Kc(v)}{R_{\theta_j}(v)} \right)_{\text{calc}} \right]^2 \quad (7)$$

This rearrangement is very similar in form to the Zimm plot commonly used in light scattering. To obtain molecular weight information from a Zimm

plot, double extrapolation to zero angle and zero concentration is required. For the low concentrations used in SEC, the molecular weight can be obtained simply from the intercept of the inverse Debye plot at zero angle. The inverse Debye plot [eq. (7)] is a good approximation<sup>4</sup> over a wider range of concentrations than is its reciprocal expression [eq. (4)].

Again, regression can be used to determine both  $M_w$  and  $r_g$  at each retention volume,  $v$ . If the error is constant for each angle at a particular retention volume  $v$ , then we may be able to again use a weighting factor of unity in minimizing the "objective function". Alternatively, weighting factors reflecting the precision of the dependent variable in the fit could be calculated as the inverse of the error variance of  $[Kc(v)/R_{\theta_j}(v)]_{\text{exp}}$  from replicate data (in a similar way as was described for the Debye plot equation). However, in this case, the contribution of the error variance of the concentration to the error variance of the group was assumed to be much less than the contribution of  $R_{\theta_j}(v)_{\text{exp}}$ . Thus, realizing again that a constant value of concentration is used during any one fit, the required weighting factor for eq. (7) at a particular  $v$  could be calculated from

$$w_j = \frac{R_{\theta_j, \text{exp}}^4}{s_{\text{exp}}^2} \quad (8)$$

for each of the different angles,  $j$ . In this paper, fits were done using the inverse Debye plot equation with this weighting factor as well as with the more traditional weighting factor of unity.

### The "No-rearrangement" Equation

Finally, considering that both the Debye and inverse Debye equations actually originate from a desire to obtain straight-line graphs, and since regression is being used here and such graphs are not required, yet another alternative is to avoid rearrangement completely and to fit just the light-scattering signal, minimizing

$$Q = \sum_{j=1}^{n_a} w_j ([R_{\theta_j}(v)]_{\text{exp}} - [R_{\theta_j}(v)]_{\text{calc}})^2 \quad (9)$$

where the weighting factor is

$$w_j = \frac{1}{s_{\text{exp}}^2} \quad (10)$$

Note that the error in concentration makes no contribution to the weighting factors because only  $R_{\theta_j}(v)$

is being fitted. As before, concentration is a single, constant value during a fit. With eq. (1) as the basic equation for the analysis and assuming that the difference in the errors with angle are similar (i.e., no significant influence of weighting factors), the result of using eq. (9) should provide the same results as using eq. (4). However, straight-line plots no longer are obtained using eq. (4) [or eq. (9) for that matter] if additional terms are used in the expression for  $P(\theta)$  [eq. (2)]:

$$P(\theta) \simeq 1 - \frac{16\pi^2 n_0^2 r_g^2(v) \sin^2(\theta/2)}{3\lambda_0^2} + \frac{16^2 \pi^4 n_0^4 r_g^4(v) \sin^4(\theta/2)}{12\lambda_0^4} \quad (11)$$

or if more complex expressions than eq. (1) are used for the light-scattering response:

$$R_\theta(v) = \frac{K c(v)}{1} + 2A_2 c(v) \quad (12)$$

$$P(\theta) M_w(v)$$

where  $A_2$  is the second virial coefficient.

Equation (12) is a form that has provided motivation for using the inverse Debye plot equation since it can be rearranged to a straight-line form:

$$\frac{K c(v)}{R_\theta(v)} = \frac{P^{-1}(\theta)}{M_w(v)} + 2A_2 c(v) \quad (13)$$

However, it should be reiterated that estimates of  $r_g$  and  $M_w$  at each retention volume no longer require graphical solutions. In this paper, linear regression easily handles curves generated using eq. (11) with eq. (4) or (9), for example.<sup>‡</sup> Equation (9) was used only with eq. (11) (i.e., not with fewer terms) in this work. Examination of the ability of one equation to handle a more complicated form than the other for a graphical solution is not the subject of this work. Rather, we will show the results obtained from eqs. (4), (7), and (9) applied in a variety of ways using regression and on data where they may be expected to arrive at the same estimates of  $r_g$  and  $M_w$  at each retention volume. Two aspects are examined: the degree of fit to the data obtained and the precision of the estimates of  $r_g$  and  $M_w$  obtained at each

retention volume. These are discussed in the next section.

## STATISTICAL MEASURES

### Degree of Fit

A plot of residuals (i.e., the difference between the calculated ordinate value and the experimental ordinate value) vs.  $\sin^2(\theta/2)$  can be used to scrutinize any systematic lack of fit of eq. (2) to the data. Such a plot shows the difference between the fitted value and the experimental data. These were used in this work along with an analysis of variance to check adequacy of fit.<sup>5</sup> The latter method tests for lack of fit by comparison of the ratio of the sum of squares due to both lack of fit and sum of squares due to pure error to the  $F$ -distribution. A simple "yes" or "no" can then be tabulated to specify whether or not lack of fit was significant at the 90% level. Details of the computation method are in standard statistics references.<sup>5,6</sup>

### Precision of $M_w$ and $r_g$

Defining the error in  $M_w$  and  $r_g$  allows for the interdependence of these two calculated quantities. Previous studies have ignored this interdependence. Accounting for it requires calculation of joint confidence regions (JCRs) rather than simple confidence intervals based upon standard deviations.<sup>7-9</sup> A JCR is shown as a closed area on a plot of  $M_w$  vs.  $r_g$ . Its meaning can best be understood by stating that if 100 replicate sets of data are each analyzed to provide a 95% joint confidence region, then, in approximately 95 of the 100 regions so obtained, the true value of  $M_w$  and  $r_g$  will be represented by a point inside the region, and in about five cases, the true values will fall outside. In contrast, the more traditional calculation of a 95% confidence interval appears as a defined range of values for either  $M_w$  or  $r_g$  and assumes that  $M_w$  is independent of  $r_g$ . For  $M_w$ , for example, this means that if  $M_w$  is independent of  $r_g$  and if 100 replicate measures of  $M_w$  are each analyzed to provide a 95% confidence interval, then, in approximately 95 of the 100 intervals so obtained, the true value of  $M_w$  will be represented by a point inside the range, and in about five cases, the true value will fall outside. It is well known that two coefficients in an equation (e.g.,  $M_w$  and  $r_g$  in this case) are generally not independent. Furthermore, when the independence assumption is not valid, then the 95% confidence intervals are known to be much inferior to the JCR in defining precision. This will be shown graphically in a later section.

<sup>‡</sup> Note that linear regression refers to linearity in the equation coefficients and not linearity in the independent variable,  $\sin^2(\theta/2)$ . Therefore, linear regression programs can fit both straight lines and some curves (e.g., polynomials).

The traditional confidence interval for a mean value is the product of the standard deviation of the mean and the appropriate value from the Student's *t* distribution.<sup>5,7</sup> An estimate of the interval for a single measurement is of interest here and is considered as  $\pm 2s$ , where *s* is the sample estimate of the standard deviation. Calculation of joint confidence regions is more difficult but still readily accomplished. Several methods are available. A general method involving nonlinear regression was used here.<sup>9</sup>

## EXPERIMENTAL CONDITIONS

Experimental conditions were as described in Part I.

## COMPUTATIONAL METHODS

The differential refractive index used was 0.184 mL/g for polystyrene at 40°C in tetrahydrofuran. For polyethylene in 1,2,4-trichlorobenzene (TCB) at 145°C, the value of the differential refractive index increment used was -0.098 mL/g based on work done by Grinshpun.<sup>10</sup> Joint confidence regions calculated to estimate precision were done using the Nelder-Mead<sup>11</sup> simplex optimization method. Statistical procedures in the SAS computer program were used to evaluate lack of fit and significance of parameters.

## RESULTS AND DISCUSSION

### Degree of Fit

To verify that the models chosen for the multiangle data were adequate, statistical tests were performed using the 10 repeated SEC/MALLS measurements. Analysis of variance for the repeated SEC/MALLS measurements was used to assess the lack of fit at four different retention volumes for both the high- and room-temperature data. Three basic equations were used: (i) eq. (9) with no rearrangement; (ii) eq. (4), the Debye plot; and (iii) eq. (7), the inverse Debye plot equation. All weighting factors were set at unity in the lack of fit test. The number of terms carried in the  $P(\theta)$  or  $P^{-1}(\theta)$  expressions [eqs. (2) and (6)] determined the order of the polynomial. Not all of the data from the 15 possible detector angles were used because usually the lowest angles showed excessive noise. Several sets of detector angles were considered in the analysis and they are listed in Table I. The results from SAS are summarized in Tables II and III. When only four angles

were used, they were chosen based on the most reproducible signal (smallest standard deviation).

For the room-temperature MALLS results listed in Table II, the four retention volumes selected correspond to molecular weights ranging from 175,000 to 700,000. Lack of fit of the linear models was not significant at the 90% level despite the use of different equations or various combinations of angles. However, the percent variation explained by the model improved notably (e.g., from 33 to 99% in one case) when the lowest angle was omitted from the calculations. When only the most precise four angles were used, a reasonably high percentage, i.e., 50–90%, of the variation in the data was explained by the linear models; however, the degree of freedom on the lack of fit error sum of squares was only 1 when four angles were used. Thus, the analysis of variance would not be very sensitive to the lack of

Table I MALLS Detector Sets Used

Temperature (°C)	Detector Set	No. Angles	Actual Observation Angles
145	I	15	13.4°, 21.0°, 28.2°, 35.8°, 44.2°, 53.8°, 64.8°, 77.0°, 90.0°, 103.0°, 115.2°, 126.2°, 135.8°, 144.2°, 151.8°
	II	13	28.2°, 35.8°, 44.2°, 53.8°, 64.8°, 77.0°, 90.0°, 103.0°, 115.2°, 126.2°, 135.8°, 144.2°, 151.8°
	III	4	44.2°, 53.8°, 77.0°, 115.2°
40	IV	15	20.2°, 27.7°, 35.4°, 43.9°, 53.6°, 64.7°, 76.9°, 90.0°, 103.1°, 115.4°, 126.4°, 136.1°, 144.6°, 152.3°, 159.8°
	V	14	27.7°, 35.4°, 43.9°, 53.6°, 64.7°, 76.9°, 90.0°, 103.1°, 115.4°, 126.4°, 136.1°, 144.6°, 152.3°, 159.8°
	VI	4	53.6°, 136.1°, 152.3°, 159.8°

**Table II Room-temperature MALLS Lack of Fit Assessment**

Retention Volume (mL)	Eq. No.	Description	Model <sup>a</sup>	No. Angles	Percent Variation Explained by Model	Lack of Fit Significant at 90% Level
17.4 ( $M_w$ 697,000)	(9)	Not rearranged	$y = a + bx + cx^2$	15	60.00	No
				14	99.90	No
				4	65.00	No
18.4 ( $M_w$ 437,000)	(9)	Not rearranged	$y = a + bx + cx^2$	15	33.00	No
				14	99.70	No
				4	72.80	No
	(4)	Debye	$y = a + bx$ $y = a + bx + cx^2$ $y = a + bx$	14	99.99	No
				14	99.95	No
				4	83.60	No
	(7)	Inverse Debye	$y = a + bx$ $y = a + bx + cx^2$ $y = a + bx$	14	99.99	No
14				99.98	No	
4				83.40	No	
19.4 ( $M_w$ 270,000)	(4)	Debye	$y = a + bx$	15	99.00	No
				14	99.98	No
				4	90.40	No
20.4 ( $M_w$ 175,000)	(4)	Debye	$y = a + bx$	15	99.00	No
				14	98.20	No
				4	54.50	No

<sup>a</sup>  $x = \sin^2(\theta/2)$  for all equations used—eq. (9):  $y = R_\theta$ ; eq. (4):  $y = R_\theta/(Kc)$ ; eq. (7):  $y = (Kc)/R_\theta$ .

fit in the four-angle case. Adding higher-order terms in the expressions did not improve the fit. Thus, for a linear homopolymer, such as the NBS 706, first-order equations gave adequate representation of the light-scattering effects. For optimum results, the lowest angle should not be included in calculations for the molecular parameters of interest.

The high-temperature MALLS results are listed in Table III. Here, the four retention volumes correspond to molecular weights ranging from 15,000,000 to 86,000. Lack of fit of the linear model was significant for some of the retention volumes despite the different equations or various combination of angles. The percent variation explained by the model improved only marginally even when the lowest two angles were omitted from the calculations. When only the most precise four angles were used, a reasonably higher percentage ( $\sim 50\%$ ) of the variations in the data is explained by the linear models. For the peak of the chromatogram (34.13 mL), additional terms were included in the  $P(\theta)$  or  $P^{-1}(\theta)$ , leading to higher-order polynomials being used. Using higher polynomials did improve the fit, especially going from first- to second-order polynomials. The cubic equation offered a smaller im-

provement relative to the second-order expression.

Comparing Tables II and III, it can readily be seen that modeling high-temperature MALLS proved a much more challenging task than did modeling the room-temperature data. As expected, the light-scattering signal was weaker than that obtained at room temperature. Also, there were more sources of error; for example, temperature fluctuation perturbed the differential refractive index increment. For a branched polymer, such as the SRM 1476, higher terms may be required for adequate representation of the light-scattering effects. However, noise levels in these data were too high to permit this aspect to be examined. Omitting the two lowest angles, i.e., using either detector set II or III (listed in Table I) for the high-temperature MALLS data, gave better fit than if these angles were included in the regression calculation. However, even the very best fit obtained explained only 65% of the variation in the data.

#### Precision of $M_w$ and $r_g$

As mentioned previously, confidence intervals calculated from the standard deviation can be inadequate estimates of precision because of the inter-

**Table III High-temperature MALLS Lack of Fit Assessment**

Retention Volume (mL)	Eq. No.	Description	Model <sup>a</sup>	No. Angles	Percent Variation Explained by Model	Lack of Fit Significant at 90% Level	
30.8 ( $M_w$ 15,000,000)	(9)	Not rearranged	$y = a + bx + cx^2$	15	00.00	Yes	
				13	43.40	No	
				4	14.40	No	
32.5 ( $M_w$ 523,000)	(9)	Not rearranged	$y = a + bx + cx^2$	15	0.01	Yes	
				13	3.30	Yes	
				4	46.00	No	
34.1 ( $M_w$ 154,000)	(9)	Not rearranged	$y = a + bx + cx^2$	15	0.04	Yes	
				13	0.75	Yes	
				4	50.00	No	
	(4)	Debye	$y = a + bx$	13	5.43	Yes	
				$y = a + bx + cx^2$	13	21.60	No
				$y = a + bx + cx^2 + dx^3$	13	30.60	No
				$y = a + bx$	4	57.20	No
	(7)	Inverse Debye	$y = a + bx$	13	3.60	Yes	
				$y = a + bx + cx^2$	13	19.70	No
				$y = a + bx + cx^2 + dx^3$	13	29.90	No
35.0 ( $M_w$ 86,000)	(9)	Not rearranged	$y = a + bx + cx^2$	15	0.12	Yes	
				13	1.25	Yes	
				4	8.00	Yes	

<sup>a</sup>  $x = \sin^2(\theta/2)$  for all equations used—eq. (9):  $y = R_\theta$ ; eq. (4):  $y = R_\theta/(Kc)$ ; eq. (7):  $y = (Kc)/R_\theta$ .

dependence among parameters. Such is the case for MALLS when both  $r_g$  and  $M_w$  are determined from the same equation. In Figure 1, lines representing two standard deviations (approximate 95% confidence limits) are shown superimposed on the corresponding joint confidence region (JCR). If the correlation between  $r_g$  and  $M_w$  is ignored, a rectangle is obtained. The precision defined by the JCR shows that this rectangle encloses some area not included by the JCR and fails to include some area that is included by the JCR. Thus, to accurately represent the 95% confidence level of the derived parameters using MALLS, joint confidence regions were used instead of standard deviations. Plots of residuals are also included to investigate any vital differences between the models and the degree of fit.

JCRs were found for each of the options outlined in the theory section. Two different sets of scattering angles were used in the calculations at both room and high temperature. Figure 2 is a plot of the standard deviation of  $R_\theta$  vs. scattering angle at room

temperature. The 14 points shown correspond to one set of angles (detector set V in Table I) used to find  $M_w$  and  $r_g$ . The second set of angles used to calculate  $M_w$  and  $r_g$  were the most precise four angles shown in Figure 2 (detector set VI). Figure 3 is the same plot for the high-temperature MALLS data. The two sets of angles used to determine  $r_g$  and  $M_w$  are detector sets II and III (see Table I). Detector set III is indicated by the unfilled squares plotted in Figure 3. In the following sections, selection of the appropriate equations to be used is discussed at both room and high temperatures.

### Room Temperature

The JCRs are plotted along with the various estimates of local  $M_w$  and  $r_g$  obtained at a single value of retention volume in Figures 4 and 5. The retention volume of 18.4 mL was chosen here because it corresponds to the peak of the chromatogram. The use of only four angles considerably shortens calculation

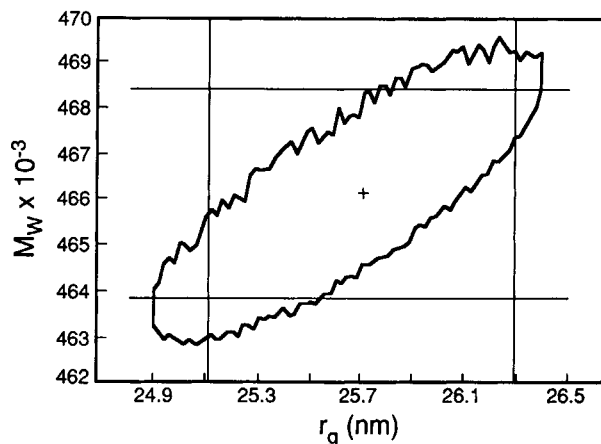


**Figure 1** 95% confidence intervals (defined by the rectangle) compared with the corresponding JCR (the ellipse) for local weight-average molecular weight and local radius of gyration determined by SEC/MALLS. Results are from use of the Debye equation at a retention volume of 18.4 mL and collection from 14 scattering angles.

time and allows selection of only the most precise angles. However, the JCRs show that estimates of local  $M_w$  and  $r_g$  obtained from using only four angles (Fig. 5) are less precise than those obtained from using 14 angles (Fig. 4) because the four angles are not sufficiently near to the intercept ( $54^\circ$ – $160^\circ$  compared with  $28^\circ$ – $160^\circ$ ).

Plots of residuals for all methods showed a random scatter regardless of whether weighted or unweighted residuals were plotted. From examination of the plot of standard deviation vs.  $\theta$  (Fig. 2), it was evident that the error was almost constant with the angle except for the very lowest angle used and it was just barely significantly higher than the oth-

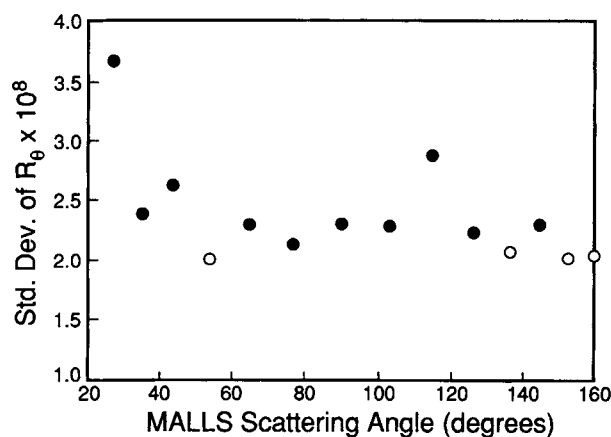


**Figure 2** MALLS detector precision at room temperature for a retention volume of 18.4 mL for SEC/MALLS (open circles correspond to angles providing most precise MALLS detector signal).

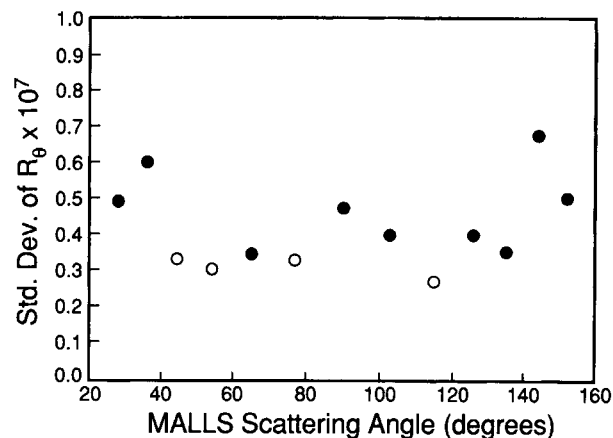


**Figure 3** MALLS detector precision at high temperature for a retention volume of 34.1 mL for SEC/MALLS (open circles correspond to angles providing most precise MALLS detector signal).

ers. The lack of effect of weighting factors on the random pattern of the scatter in plots of residuals was attributed to this invariance of error with angle.

Considering the results of using eqs. (4) (the Debye plot) and eq. (9) (the "no-rearrangement" alternative), both indicated equivalent precision (identical joint confidence regions) for local  $M_w$  and  $r_g$  regardless of the detector set used. The main difference between the above two options is the error in the ordinate because concentration was not included in the ordinate of one, but is in the other. In the regression, only a first-order term is required in eq. (5) because it gave adequate representation for linear homopolymers. Plotting the JCR from the

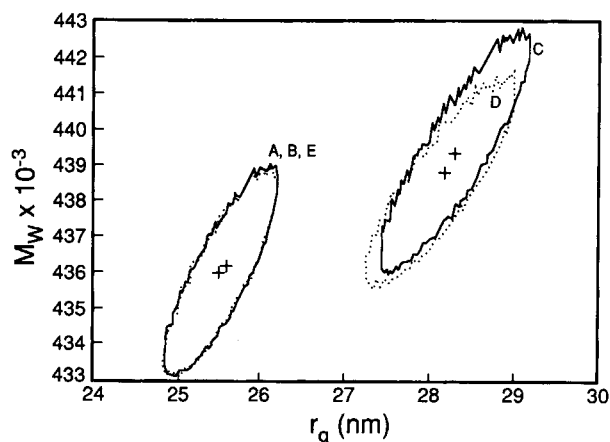


**Figure 4** JCRs for local weight-average molecular weight and local radius of gyration for room-temperature MALLS using 14 angles (SEC/MALLS, NBS 706 polystyrene analysis at 18.40 mL): (A) Debye; (B) weighted Debye; (C) inverse Debye; (D) weighted inverse Debye; (E) unrearranged equation; (+) best estimate.



Debye plot equation with weighted regression also yielded the same JCR.

In contrast to the other two equations, the unweighted inverse Debye plot [eq. (7)] appeared inferior to the other methods in precision. Also, the estimates of  $r_g$  and  $M_w$  obtained from eq. (7) were quite different than those obtained from either of the other two equations. In the inverse Debye plot equation, the linear approximation used for the  $P^{-1}(\theta)$  shifted the  $r_g$  and  $M_w$  estimated to higher values compared to the Debye plot case, because the approximation becomes inadequate for large molecules or high angles. For MALLS data, a greater number of high-scattering angles were available. Use of the more correct weighting factor [eq. (8)] did provide a smaller joint confidence region than that obtained when all detector angles were treated equally for the four-angle detector set (Fig. 5) because the lowest angle was weighted the most (smallest standard deviation). However, it was found, again, that of all the equation options, the inverse Debye plot is the most sensitive to the precision of the lower angles. Removal of the assumption that concentration error did not contribute to the weighting factor was not examined; its removal may well improve the results for this equation still more. However, the need to specify weighting factors extremely accurately for this equation was considered such a liability that further computational development work with the equation was not pursued.

Hence, the linear unweighted (all angles treated equally) Debye equation was used in the analysis of

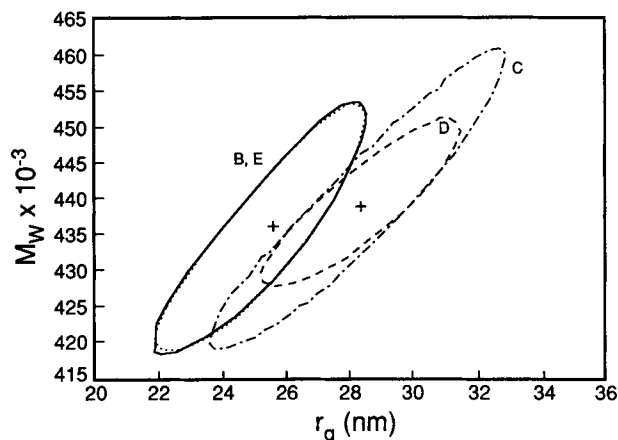


**Figure 5** JCRs for local weight-average molecular weight and local radius of gyration for room-temperature MALLS using only most precise four angles (SEC/MALLS, NBS 706 polystyrene analysis at 18.40 mL): (A) Debye; (B) weighted Debye; (C) inverse Debye; (D) weighted inverse Debye; (E) unrearranged equation; (+) best estimate.

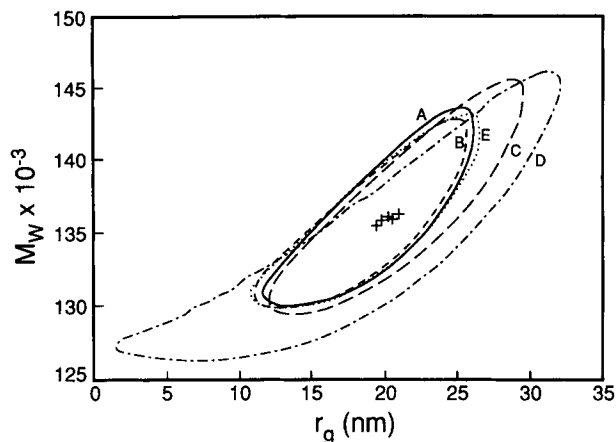


**Figure 6** JCRs for local weight-average molecular weight and local radius of gyration for high-temperature MALLS (SEC/MALLS, SRM 1476 low-density polyethylene analysis at 34.13 mL): (A) Debye; (B) weighted Debye; (C) inverse Debye; (D) weighted inverse Debye; (E) second-order equation; (+) best estimate.

the NBS 706 MALLS data in Part I of this study over the inverse Debye and the “not-rearranged” equations. It produced  $r_g$  and  $M_w$  of equal or better precision and was more “robust” in terms of reduced sensitivity to the actual detector angles used in the regression compared to the inverse Debye case. The “not-rearranged” equation [eq. (9)], which utilized the Nelder–Mead simplex search routine to find  $r_g$  and  $M_w$ , required a much longer computation time. Introducing weighting factors based on the error variance at each angle did not offer any gain in precision of the molecular parameters calculated using the Debye equation for the room-temperature SEC/MALLS system.

### High Temperature

The JCRs for  $r_g$  and  $M_w$  at 34.1 mL are plotted in Figures 6 and 7. At 34.1 mL, the chromatogram of the main polymer peak of SRM 1476 showed the strongest signal. The 95% confidence region for the  $r_g$  value at high temperature ranged from 2 to 33 nm, and, therefore,  $r_g$  was considered not reproducible regardless of the equation used. In contrast, the  $M_w$  value showed an acceptable range of 127,000–147,000 at the 95% confidence level. When only the four most precise angles were used (Fig. 7), precision of both  $r_g$  and  $M_w$  decreased from the case when 13 angles were included in the calculations (Fig. 6), with the effect being particularly acute for  $r_g$ . Similar to the results of the room-temperature study, the four angles selected were not sufficiently near to the intercept for a precise estimate of  $M_w$  to be obtained.

For the number of points available, no systematic

variation was detected from the plots of residuals for any of the equations regardless of whether weighted or unweighted residuals were plotted. From examining the plot of the standard deviation vs.  $\theta$  (Fig. 3), it can be seen that the error variation with respect to detector angle was slight.

JCRs from eq. (4) (the Debye plot) and eq. (9) combined with eq. (11) (the second-order polynomial) demonstrated similar precision for local  $M_w$  and  $r_g$  regardless of the detector set used. Including the second-order term in the expansion for  $P(\theta)$  did not improve the precision, i.e., the JCR was not altered. The JCR from the Debye plot with weighting factors used in the regression showed only a marginal improvement over the others.

The inverse Debye plot [eq. (7)] again appeared inferior to the other methods in terms of precision at high temperature as well as room temperature. The estimated  $r_g$  and  $M_w$  were shifted to higher values compared to the Debye plot case, but, in general, there is a good grouping in the estimated values for  $r_g$  and  $M_w$  considering the uncertainty involved in the data. Use of the experimentally determined weighting factors [eq. (8)] revealed larger JCRs compared with when all detector angles were treated equally for both the four-angle and 14-angle detector sets (Figs. 6 and 7) because the highest angle was weighted the most (smallest standard deviation). Thus, again, of all the options, the inverse Debye plot is the most sensitive to the weighting factors used. A slight change in the weighting of the angles used in the regression is critical for the precision of the calculated  $r_g$  and  $M_w$ .

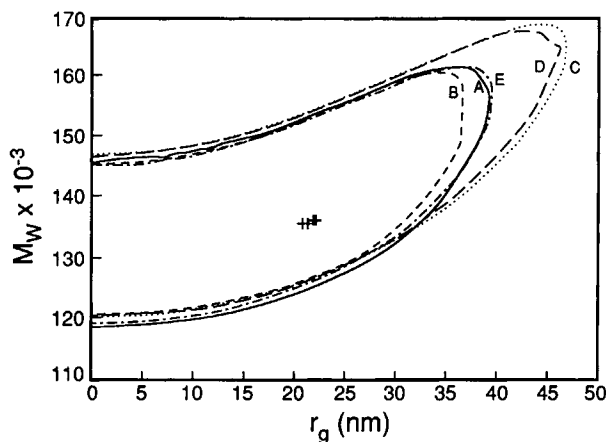


**Figure 7** JCRs for local weight-average molecular weight and local radius of gyration for high-temperature MALLS using only the most precise four angles (SEC/MALLS, SRM 1476 low-density polyethylene analysis at 34.13 mL): (A) Debye; (B) weighted Debye; (C) inverse Debye; (D) weighted inverse Debye; (E) second-order Equation; (+) best estimate.

Thus, the simple unweighted Debye equation was the appropriate equation to use for the SRM 1476 MALLS data in this study. No appreciable improvement in precision was gained by increasing the order of the equation, and introducing weighting factors based on the error variance at each angle, because the main source of imprecision was not systematic. Although the inverse Debye equation (similar to the Zimm equation) is the most common form found in the literature for classical light scattering, it is less tolerant in the selection of appropriate detector angles in the calculation. The chromatograms at low angle must be very precise in order to calculate reliable  $r_g$  and  $M_w$  using the inverse Debye equation. Higher angles can be used with the Debye equation with less serious effect.

### Correlations of $M_w$ and $r_g$

Plots of  $M_w$  vs.  $r_g$  are now commonplace in the literature.<sup>1,12</sup> These plots are done with the objective of elucidating property interrelationships in polymer molecules.<sup>12</sup> However, as seen in this work (as well as in our earlier results on different samples of the same polymer<sup>2</sup>), the JCR plots show that the "natural scatter" of  $M_w$  vs.  $r_g$  occurs in a diagonal direction along the route of such correlations. This is a consequence of experimental error in the raw data and the least-squares fitting procedure. Similar effects in other areas of chemistry resulting when the slope and intercept of straight lines were correlated have misled many investigators.<sup>13,14</sup> To avoid this result in light-scattering analysis, it is recommended that future investigations be concerned with this aspect. Also, methods of treating the data in other ways (by utilizing equations that include only one of the parameters; e.g., Ref. 15) may well provide independent estimates of  $M_w$  and  $r_g$  and should be further investigated.

### CONCLUSIONS

- In comparing the precision of  $M_w$  and  $r_g$  determined from MALLS, the correlation of errors between the two parameters needs to be taken into account. Thus, the true error in  $r_g$ , as shown in joint confidence regions, was significantly greater than that estimated from standard deviation calculations.
- Studies directed at establishing correlations between  $M_w$  and  $r_g$  should define the JCRs for their data to distinguish real effects from random error. Failure to do so has meant misleading results in analogous situations in other areas of chemistry.

- Equation selection in MALLS was found to affect both accuracy and precision of calculated results. In particular, the inverse Debye equation eq. 7 provided very different estimates of significantly lower precision than did either the Debye equation eq. 4 or the not-rearranged equation eq. 9.
- Using the most precise four detector angles did not necessarily improve the precision of the calculated values for multiangle light scattering data. The angles used must be as close to zero as possible (as well as being reasonably precise) for the intercept,  $M_w$ , and slope,  $r_g$ , to be reproducible.

## NOMENCLATURE

$c_i$	concentration at retention volume, $v_i$
$c(v)$	concentration as a function of retention volume, $v$
$dn/dc$	differential refractive index increment
$K$	optical constant defined by eq. (3)
$\bar{M}_w$	local weight-average molecular weight at some retention volume
$M_{wi}$	local weight-average molecular weight at retention volume, $v_i$
$M_w(v)$	local weight-average molecular weight as a function of retention volume
$\bar{M}_w$	whole polymer weight-average molecular weight
$N$	Avogadro's number
$n_0$	refractive index of the pure solvent
$n_a$	number of angles used in computation
$P(\theta)$	scattering function [eqs. (4) and (11)]
$P^{-1}(\theta)$	inverse scattering function [eq. (6)]
$Q$	objective function defined by eq. (5) or (7) or (9)
$R_\theta$	excess Rayleigh ratio
$R_\theta(v)$	excess Rayleigh ratio as a function of retention volume
$r_g$	whole polymer $z$ -average root mean square radius of gyration
$r_g$	local $z$ -average root mean square radius of gyration at some retention volume
$r_{gi}$	local $z$ -average root mean square radius of gyration at retention volume, $v_i$
$r_g(v)$	local $z$ -average root mean square radius of gyration as a function of retention volume
$s_{\text{exp}}^2$	error variance of $R_\theta$
$v$	retention volume
$w$	weighting factor
$\lambda_0$	wavelength of the incident light
$\theta$	scattering angle

## Subscripts

calc	calculated value
exp	experimental value
$i$	retention volume
$j$	angle

We wish to thank the Ontario Centre for Materials Research, Eastman Kodak Co., and the Natural Sciences and Engineering Research Council of Canada for grants supporting this work. Also, we wish to express our gratitude to Wyatt Technology Corp., Santa Barbara, CA, particularly to Dr. P. J. Wyatt and Ms. L. Nilsson, for providing the room-temperature MALLS data used in this study. Finally, we much appreciate the very helpful information on statistics provided by Dr. J. D. Morris of the Eastman Kodak Co.

## REFERENCES

1. C. Jackson, L. M. Nilsson, and P. J. Wyatt, *J. Appl. Polym. Sci. Appl. Polym. Symp.*, **45**, 191–202 (1990).
2. S. T. Balke, P. Cheung, L. Jeng, R. Lew, and T. H. Mourey, *J. Appl. Polym. Sci. Appl. Polym. Symp.*, **48**, 259 (1991).
3. C. Jackson, L. M. Nilsson, and P. J. Wyatt, *J. Appl. Polym. Sci. Appl. Polym. Symp.*, **43**, 99–114 (1989).
4. B. H. Zimm, *J. Chem. Phys.*, **16**(12), 1093–1099 (1948).
5. G. E. P. Box, W. G. Hunter, and J. S. Hunter, *Statistics for Experimenters: An Introduction to Design, Data Analysis, and Model Building*, Wiley, Toronto, 1978.
6. R. E. Walpole and R. H. Meyers, *Probability and Statistics for Engineers and Scientists*, 2nd ed., Macmillan, New York, 1978.
7. N. R. Draper and H. Smith, *Applied Regression Analysis*, 2nd ed., Wiley, New York, 1981.
8. L. Jeng, S. T. Balke, T. H. Mourey, L. M. Nilsson, P. J. Wyatt, P. Romeo, L. Wheeler, and A. Rudin, paper presented at the 1990 meeting of the Federation of Analytical Chemistry and Spectroscopy Societies (FACSS), Cleveland, Ohio, Oct. 5–6, 1990.
9. R. Lew, S. T. Balke, and T. H. Mourey, *J. Appl. Polym. Sci. Appl. Polym. Symp.*, **45**, 139 (1990).
10. V. Grinshpun, PhD Thesis, University of Waterloo, 1986.
11. J. A. Nelder and R. Mead, *Comput. J.*, **7**, 308 (1965).
12. P. M. Cotts, Paper presented at the 4th International Symposium on Polymer Analysis and Characterization, Baltimore, MD, May 28–31, 1991.
13. R. R. Krug, W. G. Hunter, and R. A. Grieger, *J. Phys. Chem.*, **80**, 2335 (1976).
14. S. T. Balke, *J. Appl. Polym. Sci. Appl. Polym. Symp.*, **43**, 5 (1989).
15. P. J. Wyatt, private communication to S. T. Balke, Sept. 2, 1992.

Received February 11, 1992

Accepted December 21, 1992